Dilute Solution Properties of Randomly Branched Poly(methyl methacrylate)

CHRISTIAN JACKSON,[1,*] YUAN-JU CHEN,[2] and JIMMY W. MAYS[2]

[1]Central Research and Development, E. I. du Pont de Nemours and Company, Experimental Station, Wilmington, Delaware 19880-0228, and [2]Department of Chemistry, University of Alabama at Birmingham, Birmingham, Alabama 35294-1240

SYNOPSIS

Randomly branched poly(methyl methacrylate) samples were prepared by copolymerization with different amounts of ethylene dimethacrylate. The molecular weight distributions, radius of gyration distributions, and intrinsic viscosity distributions were measured by size exclusion chromatography with refractive index, multiangle light-scattering, and viscosity detectors. The effect of branching on the radius of gyration was compared with the effect on the intrinsic viscosity. It was found that the intrinsic viscosity contraction factor g' scales with the radius of gyration contraction factor g, with the exponent, ϵ, having a value in the range 0.8–1.0. © 1996 John Wiley & Sons, Inc.

INTRODUCTION

The dilute solution properties of branched polymers have been the subject of numerous experimental and theoretical investigations.[1-4] In particular, the properties of monodisperse uniform star molecules prepared by anionic polymerization have been extensively studied and are well understood.[1] However, many materials are randomly branched during polymerization, leading to polydispersity in both molecular weight and the number of branches per molecule. It is this extreme polydispersity that, in many cases, leads to the desired change in properties compared to linear polymers. Unfortunately, this polydispersity also leads to difficulties in characterizing these materials, and the connection between branching and molecular weight polydispersity often makes it difficult to determine branching content from average properties of the polymer.

The extent of branching can be determined from the contraction of the mean-square radius of gyration $<R_G^2>$ of the polymer measured in dilute solution under θ conditions relative to the linear polymer.[5] The contraction factor is defined as

$$g = \frac{<R_G^2>_b}{<R_G^2>_l}, \quad (1)$$

where the subscripts b and l refer to the branched and linear polymers, respectively. For a sample that is polydisperse, however, scattering experiments measure the z-average mean-square radius of gyration, which has been shown to be insensitive to changes in the average degree of branching because of related changes in molecular weight polydispersity.[6]

Size exclusion chromatography (SEC) provides a convenient method for rapidly fractionating a polymer solution. For a randomly branched polymer, the fractionation will not be complete as the separation is based on hydrodynamic size. For linear polymers this does not present a problem, but for mixtures of branched and linear problems it is possible for a linear and a branched molecule to have the same hydrodynamic size but different molecular weights. Thus, they will not be separated on the chromatograph and will coelute.[7] However, for randomly branched materials this separation is adequate because branching is not uniform across the molecular weight distribution. As a result of the random polymerization process, the extent of branching increases with increasing molecular weight. There is, thus, a partial separation of

* To whom correspondence should be addressed.

Journal of Applied Polymer Science, Vol. 59, 179–188 (1996)
 CCC 0021-8995/96/010179-10

branching and molecular weight in the polymer itself.[8-10] The errors associated with this loss of resolution then are comparable to experimental errors in the measurements for low and moderate extent of branching.[11]

Recent developments in instrumentation allow SEC to be combined with light-scattering and viscosity detectors so that measurements of scattered light intensity and specific viscosity can be made directly on the eluting solution. If a multiple angle laser light-scattering detector (MALLS) is used, the radius of gyration as well as the molecular weight of each near-monodisperse eluting fraction can be determined. Thus, by comparing branched and linear samples of the same polymer the contraction factor in a good solvent, g^*, can be determined across the molecular weight distribution. In addition, the viscosity detector (Visc) can be used to determine the contraction in the intrinsic viscosity at each elution volume, defined as

$$g' = \frac{[\eta]_b}{[\eta]_l}. \qquad (2)$$

In order to clarify the relationship between good solvent measurements of g^* and g' and the predictions of the random-walk theory, a series of randomly branched poly(methyl methacrylate) (PMMA) samples with different amounts of tetrafunctional branching from ethylene glycol dimethacrylate were synthesized and characterized using SEC–Visc–MALLS. This combination of monomers gives an ideal model of randomly branched polymers as they have nearly equivalent reactivity ratios.[12] Similar polymers have been studied previously using measurements of the dilute solution properties of the whole polymer and fractions collected by solvent-nonsolvent precipitation.[12,13]

EXPERIMENTAL

Materials

Linear samples of PMMA with narrow molecular weight distributions were obtained from Polymer Laboratories (Amherst, MA) and samples with broad molecular weight distributions were obtained from American Polymer Standards (Mentor, OH).

PMMA samples having varying degrees of random branching were produced by free radical copolymerization of methyl methacrylate (MMA) with ethylene glycol dimethacrylate (EGDM). MMA (Aldrich) was dried by exposure to calcium hydride on the vacuum line, followed by distillation to remove the inhibitor. EGDM (Polysciences) was used without purification or any attempt to remove the inhibitor. It was possible to successfully utilize the inhibited EGDM directly in the radical polymerization because of the low concentrations of EGDM used. The initiator used was 2,2′-azobisisobutyronitrile (AIBN, Eastman Kodak Co.), which had been purified by recrystallization from methanol. Benzene (Fisher Scientific, Certified Grade) was used as received.

The polymerizaitons were conducted under high vacuum conditions in sealed glass reactors for 3 h at 60°C. Reactants and yields are summarized in Table I. The reaction conditions and durations used gave conversions of < 25% and avoided gel formation. After polymerization was completed the polymer was predipitated in methanol and purified by repeated dissolution into toluene, followed by precipitation into methanol (to remove residual monomer and initiator). Fractionation was conducted by incremental addition of methanol to dilute solutions (<1% w/v) of PMMA in toluene.

Size Exclusion Chromatography

The size exclusion chromatograph was a Waters 150C GPC unit (Waters Associates, Milford, MA) maintained at 30°C. A 0.2 μm filter was placed between the pump and the injector. The columns were three 300 × 7.5 mm columns packed with PLgel 20 μm MIXED-A mixed pore size particles and one 50 × 7.5 mm 20 μm packing guard column (Polymer Laboratories, Amherst, MA). The solvent was HPLC grade tetrahydrofuran without stabilizer (EM Science, Gibbstown, NJ). The sample solutions were 2 mg/mL concentration, and the injection volume was 100 μL.

Light Scattering

The light-scattering detector used in conjunction with SEC was a Model F multiangle photometer equipped with a 10 mW argon ion laser (488 nm)

Table I Polymerization Conditions of Samples

Sample	MMA, mL	EDMA, mL	Benzene, mL	AIBN, g	Yield, g
R-3-3	100	0.03	90	0.3020	22
R-3-4	120	0.07	90	0.3020	24
R-3-5	120	0.14	95	0.2998	22

and temperature control (Wyatt Technology Corporation, Santa Barbara, CA). The sample cell refractive index was 1.52. The detector was placed directly after the columns and before the refractometer. The light-scattering intensity was measured at 15 angles in the range 20° to 160°, and molecular weight and radius of gyration were determined using the method of Berry.[14] The instrument was calibrated using narrow molecular weight distribution polystyrene and poly(methyl methacrylate) standards of known molecular weight. The second virial coefficient correction to the light-scattering equation was determined to be negligible due to the very low concentrations employed. The resulting errors in the calculation of the molecular weight are less than 1% based on the values for the second virial coefficient measured by static light scattering. The specific refractive index increment of PMMA in THF was determined to be 0.089 mL/g at 488 nm and 30°C.

For the light-scattering measurements on the unfractionated solutions the instrument was a Brookhaven Instrument BI-200SM light-scattering goniometer. An argon-ion laser with wavelength 488 nm and power of 200 mW was used. Five solutions of each polymer were made ranging from 1 to 4 mg/mL. Zimm plots were used to analyze the data.

Viscosity

The viscosity detector was a Model 150R (Viscotek Corporation, Houston, TX) and was placed in series after the light-scattering detector and before the differential refractometer. The instrument was calibrated with the same PMMA standard used for the light-scattering calibration for which the drop-time intrinsic viscosity was determined.

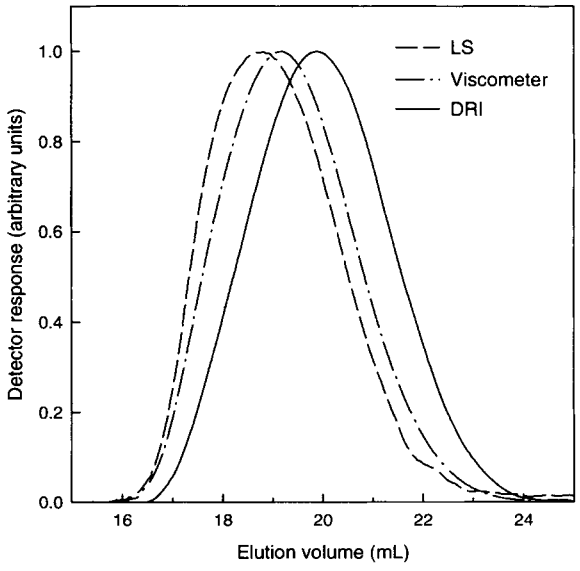

Figure 1 Chromatograph tracings for R-3-3. From left to right the signals are from the light-scattering detector, the viscometer, and the refractometer.

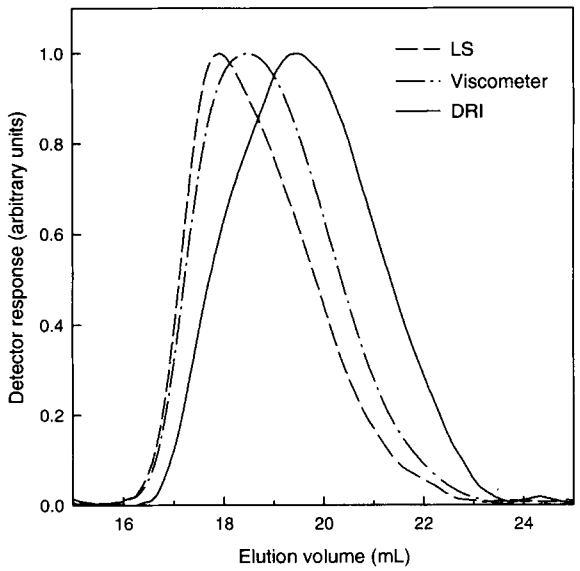

Figure 2 Chromatograph tracings for R-3-4. From left to right the signals are from the light-scattering detector, the viscometer, and the refractometer.

RESULTS AND DISCUSSION

The chromatograph tracings from the three detectors are shown in Figures 1–3 for the three branched samples. The detector signals are corrected for dead volume differences between detectors. From left to right, the peaks are light-scattering intensity, viscosity, and differential refractive index (DRI). The least branched sample, R-3-3 does not appear very different from a most probable distribution. The other two samples, however, have noticeable high molecular weight shoulders on the DRI signal tracing and a low molecular weight shoulder on the viscosity peak. The shoulder on the viscometer peak is due to the decreased sensitivity of the viscosity to branched molecules. The higher molecular weight material (lower elution volumes) in the distribution is more highly branched, the low molecular weight material (higher elution volumes) is predominantly linear. Thus, there is a decrease in sensitivity of the viscometer at the high molecular weight side of the peak. This feature can be seen in simulated viscometer chromatograms generated from the Flory–Stockmayer theory of the branched molecular weight

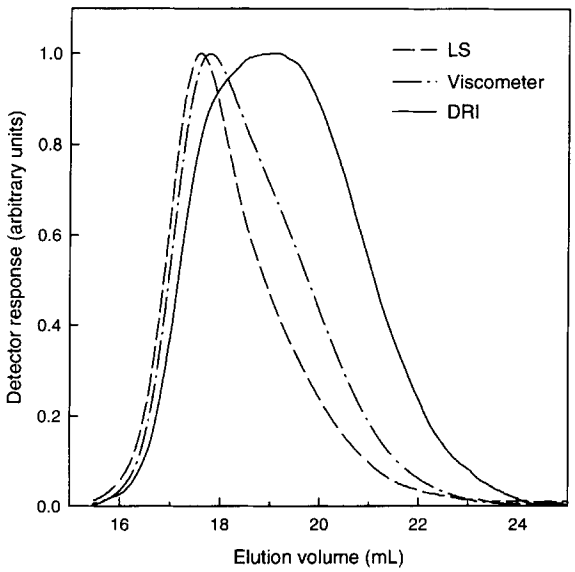

Figure 3 Chromatograph tracings for R-3-5. From left to right the signals are from the light-scattering detector, the viscometer, and the refractometer.

distribution.[11] The high molecular weight shoulder on the refractometer tracing is not predicted, however, and may be due to the size exclusion behavior of highly branched material. The volume between the different detector peak elution times increases also, indicating increased polydispersity. The molecular weights, radii of gyration, and intrinsic viscosities of the polymers measured by SEC–Visc–LS are listed in Tables II and III. The averages of the intrinsic viscosity distribution[15] are defined in terms of the weight concentration and the intrinsic viscosity of each fraction, i, of the distribution

$$[\eta]_0 = \frac{\sum c_i}{\sum c_i/[\eta]_i} \tag{3}$$

$$[\eta]_{+1} = \frac{\sum c_i[\eta]_i}{\sum c_i} \tag{4}$$

$$[\eta]_{+2} = \frac{\sum c_i[\eta]_i^2}{\sum c_i[\eta]_i} \tag{5}$$

The weight-average intrinsic viscosity $[\eta]_{+1}$ is the value determined from measurements on the unfractionated polymer solution.

Table IV shows the results from the light-scattering measurements made on the unfractionated polymer solutions. The two sets of results are in good agreement. The slightly lower value of the weight-average molecular weight obtained for the most highly branched sample (R-3-5) by SEC–LS may indicate some shear degradation of high molecular weight species on the columns.

Polymer R-3-4 was fractionated into seven fractions. Each fraction was then analyzed by SEC. Figure 4 shows the DRI tracings for the seven fractions. Equal masses were injected for each peak. Figure 5 shows the viscometer tracings and Figure 6 shows the light-scattering detector tracings. The earlier eluting, higher molecular weight peaks are broader than the lower molecular weight peaks. The difference in molecular weight can clearly be seen in the increased area under the light-scattering detector tracings for the earlier peaks. The values for the fractions of sample 4 are shown in Tables V and VI.

In order to determine the branching factors the data must be compared with values of the intrinsic viscosity and the radius of gyration for linear polymers of the same molecular weight. The molecular weight scaling relationships were determined from measurements of narrow-molecular-weight distribution PMMA standards. The Mark–Houwink coefficients were determined from measurements on seven samples in the molecular weight range 35,000 to 1,500,00 g/mol.[16]

$$[\eta] = 8.97 \times 10^{-4} M^{0.710} \tag{6}$$

in good agreement with other recently determined values.[17] The radius of gyration relationship was determined from five samples ranging from 130,000 to 1,500,000 g/mol.

$$R_G = 0.011 M^{0.596}. \tag{7}$$

Table II Results from SEC–Light-Scattering Measurements

Sample	M_n	M_w (g/mol)	M_z	M_w/M_n	M_z/M_w	R_{Gn}	R_{Gw} (nm)	R_{Gz}
Linear P-400	263,600	454,500	642,400	1.72	1.41	24.6	29.6	34.4
R-3-3	266,400	394,400	564,900	1.48	1.43	21.8	25.8	30.1
R-3-4	344,700	558,500	863,600	1.62	1.55	25.0	29.8	36.5
R-3-5	449,700	886,600	1,742,900	1.97	1.97	26.9	36.5	51.4

Table III Results from SEC–Viscometry Measurements

Sample	$[\eta]_0$	$[\eta]_{+1}$ (dL/g)	$[\eta]_{+2}$	$[\eta]_{+1}/[\eta]_0$	$[\eta]_{+2}/[\eta]_{+1}$
Linear P-400	0.660	0.848	1.032	1.28	1.22
R-3-3	0.604	0.729	0.867	1.21	1.19
R-3-4	0.724	0.879	1.044	1.22	1.19
R-3-5	0.851	1.066	1.303	1.25	1.22

The values obtained from the broad-molecular-weight distribution linear PMMA were in agreement with those obtained for the narrow standards. The values from the narrow-molecular-weight-distribution materials are more precise because a wider molecular weight range can be covered.

For each polymer sample a Mark–Houwink plot can be generated from the intrinsic viscosity and molecular weight measured at each elution volume. Figure 7 shows the Mark–Houwink plot for R-3-4. The straight line is a least-squares linear fit to the comparable data from the linear PMMA. The plot shows the expected curvature at higher molecular weights indicative of random branching. The higher molecular weight species contain more branches than lower molecular weight species and so the deviation from the linear polymer relationship increases with increasing molecular weight. A similar plot can be constructed using the values for the radius of gyration measured at each elution volume. Figure 8 shows the data from R-3-4. The data again curve away from the linear sample. From these data we can calculate the two branching factors defined by eqs. (1) and (2) as functions of molecular weight. These are shown for R-3-3, R-3-4, and R-3-5 in Figures 9, 10, and 11, respectively. In all three cases the data for the two branching factors are of similar magnitude, although the variation with molecular weight appears different. The intrinsic viscosity data are less noisy due to the greater precision of the measurement. This is most noticeable at the low molecular weight end of the data where the R_G measurement becomes increasingly noisy. The values of g' tend to be slightly higher than the values for g, except at the highest molecular weights. From the data we can calculate number-, weight-, and z-average values of the branching factors g and g'. For the radius of gyration branching factor the number-average branching index is defined as

$$g'_N = \frac{\sum_i N_i g'_i}{\sum_i N_i} \tag{8}$$

the weight-average branching index is defined as

$$g'_W = \frac{\sum_i M_i N_i g'_i}{\sum_i M_i N_i} \tag{9}$$

Table IV Results from Static Light-Scattering Measurements

Sample	M_w (g/mol)	$R_{G,Z}$ (nm)	A_2 (cm^3 mol/g^2)
Linear P-400	456,000	33.1	3.54×10^{-4}
R-3-3	382,000	30.1	3.05×10^{-4}
R-3-4	557,000	36.5	3.04×10^{-4}
R-3-5	980,000	49.9	2.92×10^{-4}

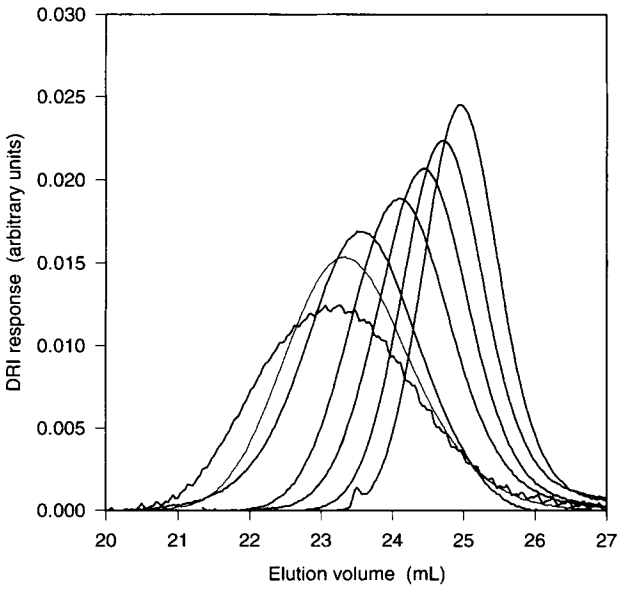

Figure 4 Differential refractometer tracings for the seven fractions of R-3-4.

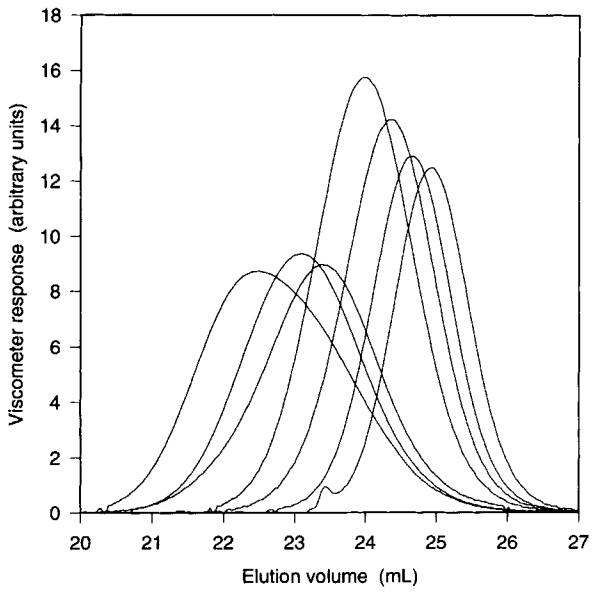

Figure 5 Differential viscometer tracings for the seven fractions of R-3-4.

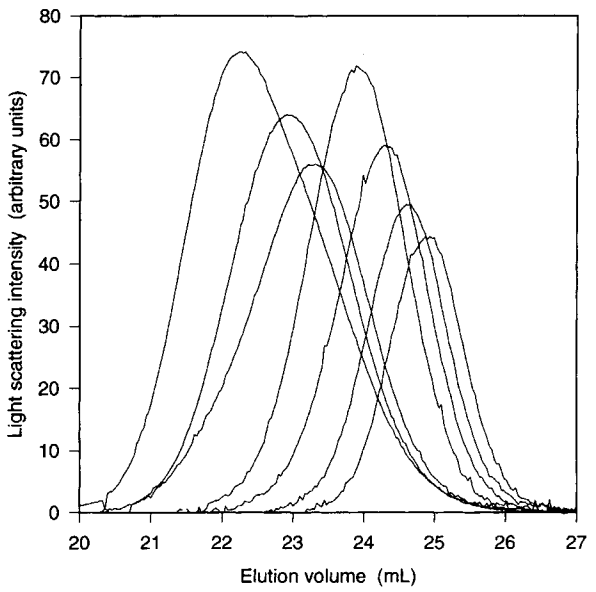

Figure 6 Light-scattering detector tracings for the seven fractions of R-3-4.

and the z-average branching index is as

$$g'_Z = \frac{\sum_i M_i^2 N_i g'_i}{\sum_i M_i^2 N_i} \qquad (10)$$

where i is the number of each elution volume element and N_i is the number of molecules in each volume element calculated from

$$N_i = \frac{M_i}{c_i}, \qquad (11)$$

where c_i is the concentration of polymer at each volume element. Similar definitions can be used for the viscosity branching factor g'. The weight- and z-average values are listed in Table VII. The number-average values are greatly affected by noise in the signals at the low molecular weight end of the distribution and tend to be unreliable. The numbers show the expected trends with the z-average values being lower than the weight-average values and decreasing values with increasing branching. The g values are consistently higher then the g' values, probably as a result of the differences in molecular-weight variation between the two factors, although the scatter in the radius of gyration values may also bias the averages.

A Mark–Houwink plot of the data for the seven fractions of R-3-4 is shown in Figure 12. In this plot, the weight-average molecular weight and intrinsic viscosities are used. The plot is similar to the one for the whole polymer in Figure 7. The linear data points shown are calculated from the molecular weight of the fractions and the Mark–Houwink coef-

Table V Results from SEC–Light Scattering for Fractions of R-3-4

Fraction	M_n	M_w (g/mol)	M_z	M_w/M_n	M_z/M_w	R_{Gn}	R_{Gw} (nm)	R_{Gz}
W-1	512,000	869,700	1,364,400	1.70	1.57	28	33	40
F-1	511,500	667,400	836,700	1.30	1.25	25	28	31
F-2	500,500	591,800	716,600	1.18	1.21	24	27	30
F-3	255,700	306,600	354,400	1.20	1.13	19	20	21
F-4	210,800	237,100	258,900	1.12	1.09	17	17	18
F-5	153,400	175,900	187,500	1.15	1.07	9	15	15
F-6	142,100	148,300	153,100	1.04	1.03	12	13	13

Table VI Results from SEC–Viscometry of Fractions of R-3-4

Sample	$[\eta]_0$	$[\eta]_{+1}$ (dL/g)	$[\eta]_{+2}$	$[\eta]_{+1}/[\eta]_0$	$[\eta]_{+2}/[\eta]_{+1}$
W-1	0.821	1.103	1.368	1.34	1.24
F-1	0.869	0.977	1.077	1.12	1.10
F-2	0.870	0.919	0.976	1.06	1.06
F-3	0.639	0.682	0.717	1.07	1.05
F-4	0.550	0.574	0.595	1.04	1.04
F-5	0.309	0.457	0.478	1.48	1.05
F-6	0.413	0.421	0.427	1.02	1.01

ficients determined for linear PMMA. Figure 13 shows a log–log plot of radius of gyration against molecular weight for the seven fractions. The data points for the weight-average radius of gyration curve away from the linear data as in Figure 8 for the whole polymer. However, the data for the z-average radius of gyration are very close to the linear polymer data. This is the value of radius of gyration that would be measured by light scattering on the fractionated polymer solutions and is the same result that was found in the earlier study,[12,13] i.e. that measurements of the z-average radius of gyration of the fractions were insensitive to branching.

The relationship between the intrinsic viscosity and radius of gyration branching factors is predicted to follow a relationship of the form

$$g' = g^{\epsilon} \tag{12}$$

where ϵ is variously predicted to be between $1/2$[18] and $3/2$.[1] The $3/2$ scaling would hold if the relationship between viscometric radius

$$R_V = \left(\frac{3[\eta]M}{10\pi N_A}\right)^{1/3} \tag{13}$$

and radius of gyration were the same for a branched as a linear chain. Lower values of the exponent indicate that the viscometric radius is less sensitive to the effect of branching than the radius of gyration. The data for the two branching factors, g and g', from the three whole polymers are shown in Figure 14 and give values of ϵ in the range 0.8–1.0. The line

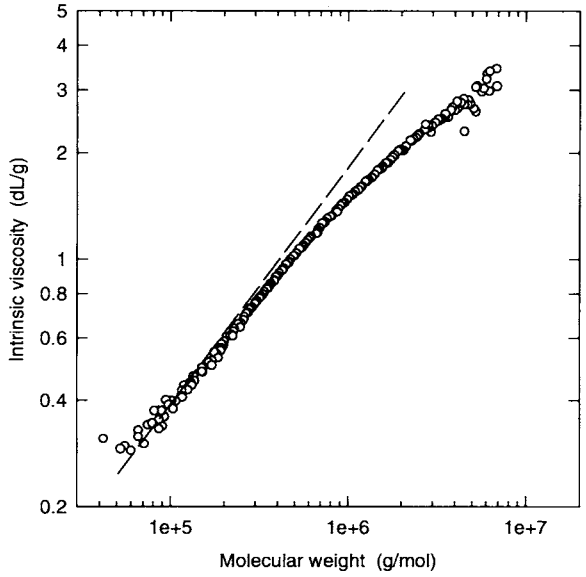

Figure 7 Mark–Houwink plot for R-3-4. The dashed line shows the Mark–Houwink relation for linear PMMA determined from the narrow-molecular-weight-distribution polymers.

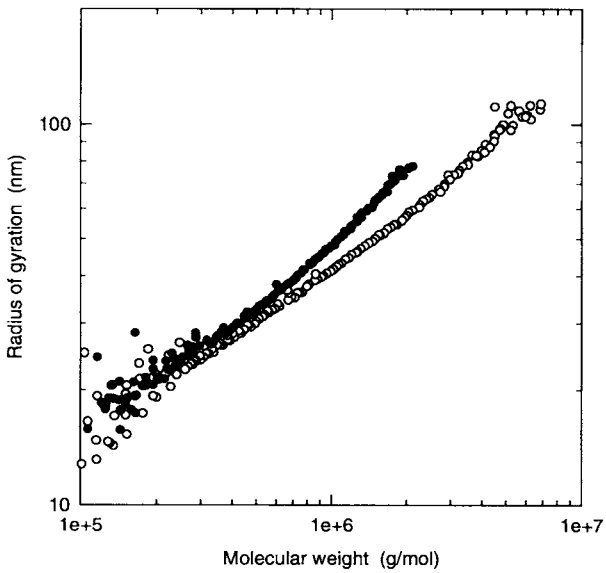

Figure 8 Plot of log radius of gyration against log molecular weight for R-3-4 (○) and for the broad-molecular-weight-distribution linear PMMA P400 (●).

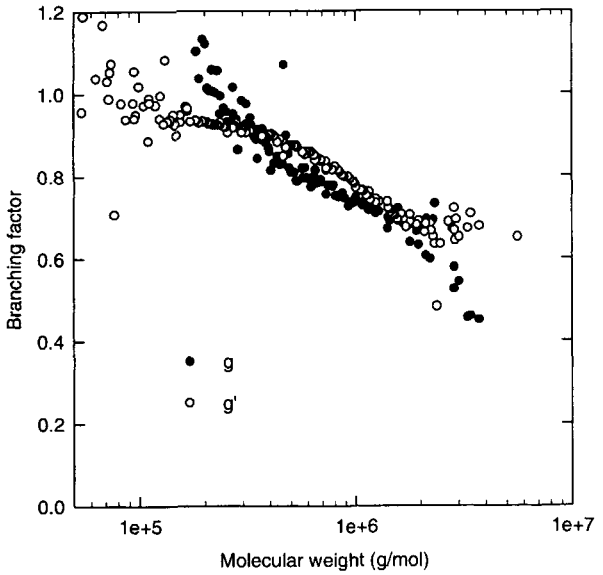

Figure 9 Plot of the radius of gyration branching factor g and the intrinsic viscosity branching factor g' against log molecular weight for R-3-3.

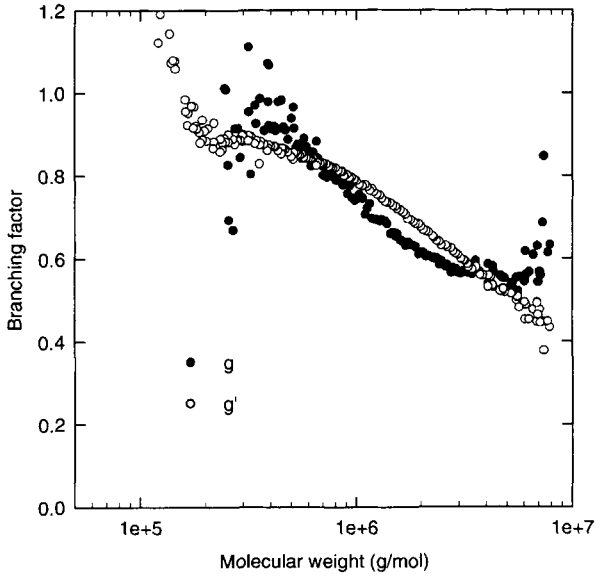

Figure 11 Plot of the radius of gyration branching factor g and the intrinsic viscosity branching factor g' against log molecular weight for R-3-5.

in Figure 14 is a least-squares fit to the data and has a slope of 0.9. The deviation from this relationship at lower values of g may be due to increased polydispersity at each elution slice at higher molecular weights. For the seven fractions of R-3-4 a plot of g' against g gives a slope of 1.0 (Fig. 15). The increase in segment density in the polymer domain due to branching, thus, changes the relationship between the viscometric size and the radius of gyration leading to a value for ϵ less than 3/2. However, for random branching, this change is not as great as it is for the extreme case of a star molecule and the exponent is, therefore, larger than 1/2.

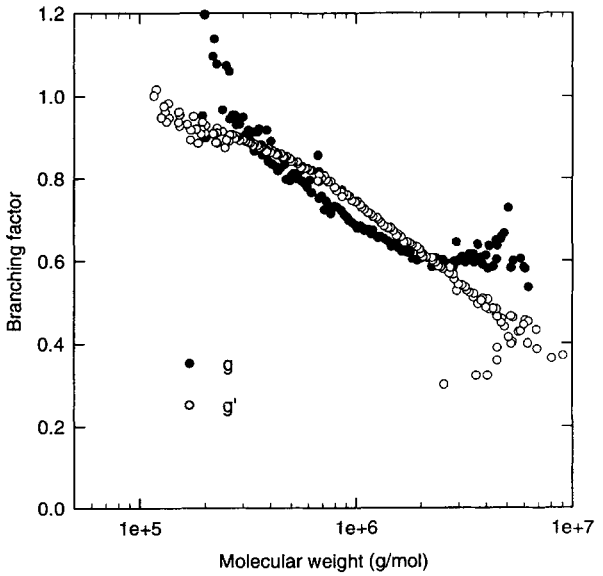

Figure 10 Plot of the radius of gyration branching factor g and the intrinsic viscosity branching factor g' against log molecular weight for R-3-4.

CONCLUSIONS

Randomly branched poly(methyl methacrylate) samples with different extent of branching were characterized using size exclusion chromatography with online light-scattering and viscosity detectors. Molecular weight, radius of gyration, and intrinsic viscosity distributions were measured. The intrinsic

Table VII Moments of the Branching Factor Distributions

Sample	g_w	g_z	g'_w	g'_z
R-3-3	0.98	0.95	0.92	0.91
R-3-4	0.97	0.93	0.89	0.85
R-3-5	0.90	0.86	0.83	0.71

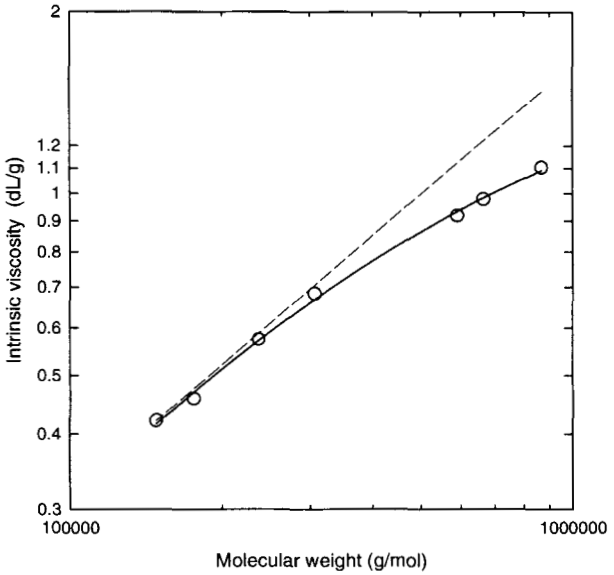

Figure 12 Mark–Houwink plot for the seven fractions of R-3-4. The dashed straight line shows the Mark–Houwink relationship for linear PMMA.

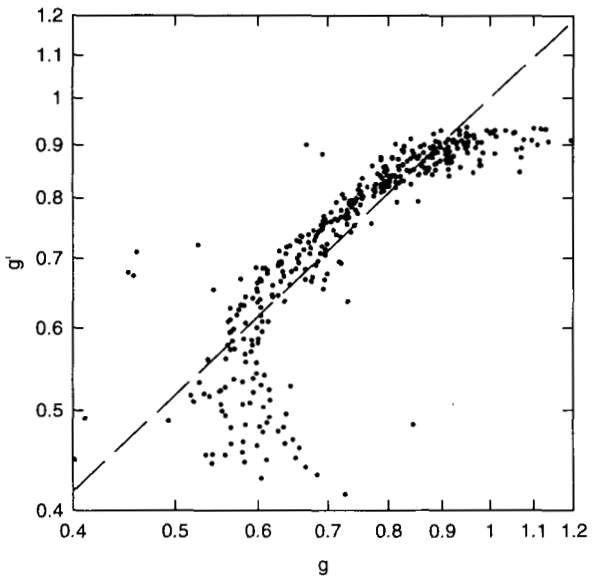

Figure 14 Log–log plot of the intrinsic viscosity branching factor g' against the radius of gyration branching factor g for R-3-5.

viscosity branching factor g' was found to be proportional to the radius of gyration branching factor with an exponent between 0.8 and 1.0. For fractions of one of the samples the exponent was found to be 0.8. If the z-average radius of gyration was measured for the fractions there was no measurable difference between the branched and linear materials.

Jimmy W. Mays thanks the E. I. du Pont de Nemours Company for financial support of the work done at UAB. We appreciate the skillful assistance of Peggy A. Ware and John B. Marshall in conducting many of the experiments.

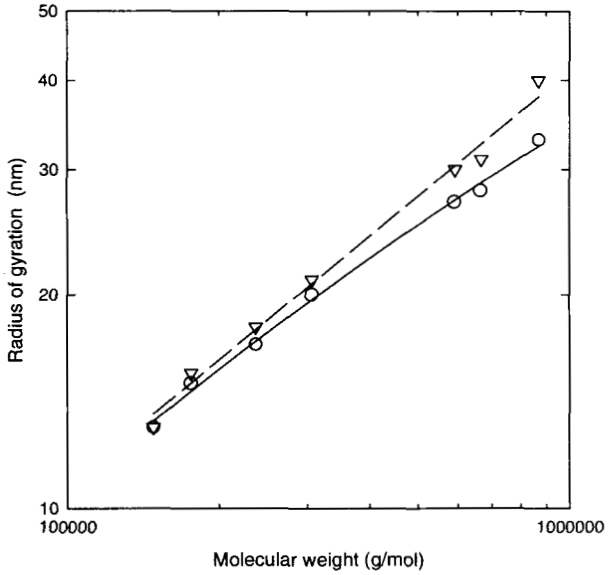

Figure 13 Plot of log radius of gyration against log molecular weight for the seven fractions of R-3-4 showing weight-average (○) and z-average (▽) values for each fraction. The dashed straight line is a fit to the data for linear PMMA.

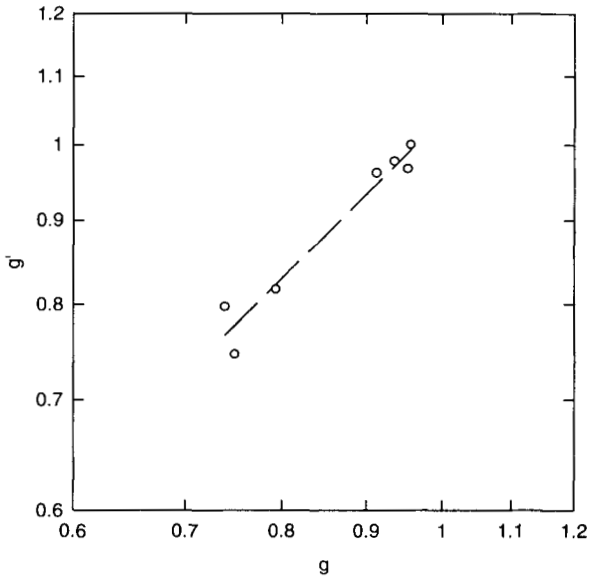

Figure 15 Log–log plot of the intrinsic viscosity branching factor g' against the radius of gyration branching factor g for the seven fractions of R-3-4.

REFERENCES

1. J. F. Douglas, J. Roovers, and K. F. Freed, *Macromolecules,* **25,** 3435 (1990).
2. P. A. Small, *Adv. Polym. Sci.,* **18,** 1 (1975).
3. J. Roovers, in *Encyclopedia of Polymer Science and Engineering,* J. Wiley & Sons, New York, 1989.
4. J. W. Mays and N. Hadjichristidis, *J. Appl. Polym. Sci.: Appl. Polym. Symp.,* **51,** 55 (1992).
5. B. H. Zimm and W. H. Stockmayer, *J. Chem. Phys.,* **17,** 1301 (1949).
6. R. W. Kilb, *J. Polym. Sci.,* **38,** 403 (1959).
7. A. Rudin, in *Modern Methods of Polymer Characterization,* H. G. Barth and J. W. Mays, Eds., John Wiley & Sons, New York, 1991.
8. W. H. Stockmayer, *J. Chem. Phys.,* **11,** 45 (1943).
9. W. H. Stockmayer, *J. Chem. Phys.,* **12,** 125 (1944).
10. P. J. Flory, *Principles of Polymer Chemistry,* Chapt. 8, Cornell University Press, Ithaca, NY.
11. C. Jackson, *J. Chromatogr.,* **662,** 1 (1994).
12. K. Kamada and H. Sato, *Polym. J.,* **2,** 489 (1971).
13. K. Kamada and H. Sato, *Polym. J.,* **2,** 589 (1971).
14. G. C. Berry, *J. Chem. Phys.,* **44,** 4550 (1966).
15. J. J. Kirkland, S. W. Rementer, and W. W. Yau, *J. Appl. Polym. Sci.: Appl. Polym. Symp.,* **48,** 39 (1991).
16. C. Jackson, Y. J. Chen, and J. W. Mays, *J. Appl. Polym. Sci.,* to appear.
17. Y. J. Chen, J. Li, N. Hadjichristidis, and J. W. Mays, *Polym. Bull.,* **30,** 575 1993).
18. B. H. Zimm and R. W. Kilb, *J. Polym. Sci.,* **37,** 19 (1959).
19. P. J. Flory and T. G. Fox, *J. Am. Chem. Soc.,* **73,** 1904 (1951).

Received November 17, 1994
Accepted July 3, 1995